

Accurate and efficient techniques for the analysis of reflection at the interfaces of three-dimensional photonic crystals

Babak Momeni,* Majid Badieirostami, and Ali Adibi

School of Electrical and Computer Engineering, Georgia Institute of Technology, Atlanta, Georgia 30332, USA

**Corresponding author: babak.momeni@osa.org*

Received July 9, 2007; accepted September 2, 2007;
posted October 10, 2007 (Doc. ID 85059); published November 12, 2007

We present two efficient and accurate models for the analysis and optimization of reflection at the interface of three-dimensional (3D) photonic crystal structures. For the most general photonic crystal interfaces, we develop a rigorous technique based on mode matching at the interface. We also explain a more efficient (yet accurate) model based on effective impedance definition for the analysis of 3D photonic crystals (PC) structures that are highly desired for practical applications. The two techniques are used to model practical 3D PC structures, and the issue of reflection minimization at the interface of such structures is addressed. © 2007 Optical Society of America

OCIS codes: 050.5298, 240.4990, 160.1245.

1. INTRODUCTION

The synthesis of optical materials with desired optical properties has been recently made possible as a result of advances in fabrication processes with subwavelength feature sizes. These attempts have resulted in the fast growing field of photonic crystals (PCs), offering unique possibilities for developing new device concepts for a broad range of applications. Activities to realize PCs have been mostly around planar structures [1] because of their compatibility with well-developed microelectronic fabrication techniques, possibility of integration in a planar platform, and their close connection to the already investigated field of integrated optics. However, there are applications including beam shaping and dispersion control in which free-space structures using three-dimensional (3D) PCs are highly preferred to avoid the issue of coupling light into and out of a planar platform. In addition, recent advances in materials and fabrication techniques such as self assembly [2], multibeam interference lithography [3–5], and multiphoton lithography [6–8] have brought the opportunity to realize high-quality 3D PCs at a low cost that can be readily used as the optical material in such applications.

While most initial applications of PCs were focused on the photonic bandgap and defect-based structures (i.e., PC waveguides and PC cavities), recently, there has been considerable interest in the application of PCs as dispersive elements. In these applications, the propagation of electromagnetic waves inside the PC is the main phenomenon of interest. In addition to detailed dispersion engineering, it is necessary to optimize the coupling of light between 3D PC structures and bulk media by appropriately modifying the interfaces to avoid unwanted reflection effects. Such reflection effects have been studied, analyzed, and proposed for the realization of practical devices in two-dimensional (2D) PC structures [9–16]. How-

ever, there has been no report on efficient analysis tools for a detailed investigation of reflection at the interfaces of common dielectric 3D PCs. For such purposes, the development of accurate and efficient methods for analysis of reflection at the interfaces of 3D PCs is necessary.

In this paper, we present two models for the detailed investigation of reflection at 3D PC interfaces. The first model (discussed in Section 2) is a rigorous analysis tool based on mode matching, and it is capable of analyzing the most general 3D PC structures. The second model that we discuss in Section 3 is based on the definition of an effective impedance for each PC mode. This effective impedance model is very efficient and accurate in analyzing reflection for cases with one dominant PC mode, which are of high interest in practical applications. We discuss the main features of the two models in Section 4. Final conclusions are summarized in Section 5.

2. RIGOROUS ANALYSIS OF REFLECTION AT PHOTONIC CRYSTAL INTERFACES

Figure 1(a) shows the geometry of the interface between a PC structure and an incident medium (usually a bulk material such as air) that is investigated in this paper. The rigorous analysis model is based on mode matching between the two regions by expanding the field at each region over Bloch modes. Phase matching condition plays a major role in describing the modes excited in the transmission region for a given incident wave. The mode-matching process also provides detailed information about the excited PC modes (e.g., penetration depth of evanescent modes as well as transmission coefficient and wave vectors of propagating modes).

We formulate the problem using the components of electric and magnetic fields tangential to the interface [i.e., E_x , E_y , H_x , and H_y in Fig. 1(a)]. Other formulations

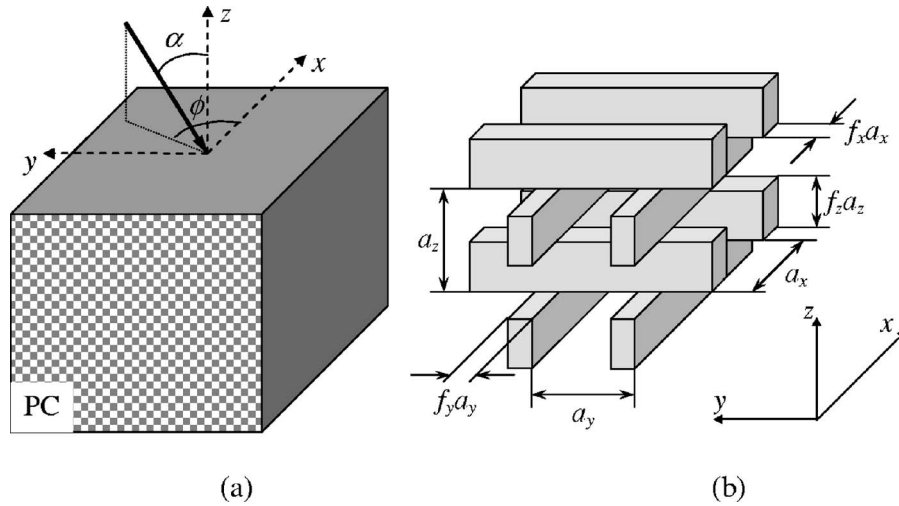


Fig. 1. (a) Setup for reflection calculation is shown, with α being the angle between the incident wave vector and the normal to the interface (z), and ϕ being the angle between the plane of incidence and xz plane. (b) Schematic of the tetragonal woodpile lattice considered throughout this paper is shown. Lattice constants and filling factors in different directions of this lattice are marked on this figure.

based on three components of the electric field or three components of the magnetic field can also be used. All these formulations are of the same order of complexity (in terms of implementation issues, required memory, and computation cost) but each might be of more interest in a particular case.

The periodic relative permittivity of the 3D PC can be represented as

$$\varepsilon_r(x, y, z) = \sum_l \sum_m \sum_n \tilde{\varepsilon}_{lmn} \exp[-j(l\mathbf{K}_1 + m\mathbf{K}_2 + n\mathbf{K}_3) \cdot \mathbf{r}], \quad (1)$$

where \mathbf{K}_1 , \mathbf{K}_2 , and \mathbf{K}_3 are the reciprocal lattice vectors of the 3D periodic structure. For these structures, the Floquet–Bloch theorem allows us to expand the magnetic and electric fields of each mode of the structure as

$$\mathbf{H}_{\mathbf{k}}(\mathbf{r}) = \sqrt{\frac{\varepsilon_0}{\mu_0}} \sum_l \sum_m \sum_n \mathbf{U}_{lmn} \times \exp[-j(\mathbf{k} + l\mathbf{K}_1 + m\mathbf{K}_2 + n\mathbf{K}_3) \cdot \mathbf{r}], \quad (2)$$

$$\mathbf{E}_{\mathbf{k}}(\mathbf{r}) = \sum_l \sum_m \sum_n \mathbf{S}_{lmn} \exp[-j(\mathbf{k} + l\mathbf{K}_1 + m\mathbf{K}_2 + n\mathbf{K}_3) \cdot \mathbf{r}], \quad (3)$$

in which \mathbf{k} is the wave vector of the mode, and \mathbf{U}_{lmn} and \mathbf{S}_{lmn} are the coefficients of different Bloch components of the magnetic and electric fields, respectively. For simplicity, we define

$$\mathbf{k}_{lmn} = \mathbf{k} + l\mathbf{K}_1 + m\mathbf{K}_2 + n\mathbf{K}_3. \quad (4)$$

To find the reflection at the interface, we use a direct mode-matching process to match the modes of the incident region to those of the PC structure at the interface. For that, we need to first find the modes of the PC structure excited by the incident wave. The next step is to

match the tangential fields at the interface to those of the incident region to find the amplitude coefficient of each mode.

Starting from Maxwell's equations:

$$\nabla \times \mathbf{E} = -j\omega\mu_0\mathbf{H},$$

$$\nabla \times \mathbf{H} = j\omega\varepsilon_0\varepsilon_r\mathbf{E}, \quad (5)$$

and expanding the fields over their Bloch components results in

$$[\mathbf{k}_y]\mathbf{S}_z - [\mathbf{k}_z]\mathbf{S}_y = k_0\mathbf{U}_x,$$

$$[\mathbf{k}_z]\mathbf{S}_x - [\mathbf{k}_x]\mathbf{S}_z = k_0\mathbf{U}_y,$$

$$[\mathbf{k}_x]\mathbf{S}_y - [\mathbf{k}_y]\mathbf{S}_x = k_0\mathbf{U}_z, \quad (6)$$

$$[\mathbf{k}_y]\mathbf{U}_z - [\mathbf{k}_z]\mathbf{U}_y = -k_0[\varepsilon]\mathbf{S}_x,$$

$$[\mathbf{k}_z]\mathbf{U}_x - [\mathbf{k}_x]\mathbf{U}_z = -k_0[\varepsilon]\mathbf{S}_y,$$

$$[\mathbf{k}_x]\mathbf{U}_y - [\mathbf{k}_y]\mathbf{U}_x = -k_0[\varepsilon]\mathbf{S}_z. \quad (7)$$

Equations (6) and (7) are obtained by inserting Eqs. (2) and (3) into the Maxwell's equations given by Eq. (5). Each component of the vector equations in Eq. (5) are written in the form of a matrix equation. The size of these matrices is $N_1 \times N_2 \times N_3$ in each dimension, where N_1 , N_2 , and N_3 are the number of Bloch orders retained in the plane-wave expansion of the fields for each reciprocal lattice vector. In these equations, the wave vector matrices are diagonal matrices with diagonal elements $([\mathbf{k}_u])_{(l,m,n)} = (\mathbf{k} + l\mathbf{K}_1 + m\mathbf{K}_2 + n\mathbf{K}_3) \cdot \hat{\mathbf{u}}$ (with $u = x, y, \text{ or } z$), and the periodicity matrix, $[\varepsilon]$, is defined as

$$([\varepsilon])_{(l,m,n),(q,r,s)} = \tilde{\varepsilon}_{(l-q)(m-r)(n-s)}. \quad (8)$$

Note that the ordered set of numbers (l, m, n) represents one of the Bloch components and a unique indexing scheme using $C = l + mN_1 + nN_1N_2$ is utilized to uniquely

address each of them. Combining Eqs. (6) and (7) to eliminate \mathbf{U}_z and \mathbf{S}_z components and assuming $[\boldsymbol{\eta}] = [\boldsymbol{\varepsilon}]^{-1}$ results in

$$-\frac{1}{k_0}[\mathbf{k}_y][\boldsymbol{\eta}][\mathbf{k}_x]\mathbf{U}_y - [\mathbf{k}_y]\mathbf{U}_x - [\mathbf{k}_z]\mathbf{S}_y = k_0\mathbf{U}_x,$$

$$[\mathbf{k}_z]\mathbf{S}_x + \frac{1}{k_0}[\mathbf{k}_x][\boldsymbol{\eta}][\mathbf{k}_x]\mathbf{U}_y - [\mathbf{k}_y]\mathbf{U}_x = k_0\mathbf{U}_y,$$

$$\frac{1}{k_0}[\mathbf{k}_y][\mathbf{k}_x]\mathbf{S}_y - [\mathbf{k}_y]\mathbf{S}_x - [\mathbf{k}_z]\mathbf{U}_y = -k_0[\boldsymbol{\varepsilon}]\mathbf{S}_x,$$

$$[\mathbf{k}_z]\mathbf{U}_x - \frac{1}{k_0}[\mathbf{k}_x][\mathbf{k}_x]\mathbf{S}_y - [\mathbf{k}_y]\mathbf{S}_x = -k_0[\boldsymbol{\varepsilon}]\mathbf{S}_y. \quad (9)$$

The set of relations in Eq. (9) can be rewritten to form an eigenvalue problem for k_z . For this purpose, we define $[\mathbf{k}_z] = k_z + [\mathbf{K}_z]$ to obtain

$$[\mathbf{M}] \begin{pmatrix} \mathbf{U}_x \\ \mathbf{U}_y \\ \mathbf{S}_x \\ \mathbf{S}_y \end{pmatrix} = k_z \begin{pmatrix} \mathbf{U}_x \\ \mathbf{U}_y \\ \mathbf{S}_x \\ \mathbf{S}_y \end{pmatrix}, \quad (10)$$

where

$$[\mathbf{M}] = \begin{pmatrix} -[\mathbf{K}_z] & \mathbf{0} & -\frac{1}{k_0}[\mathbf{k}_x][\mathbf{k}_y] & \frac{1}{k_0}[\mathbf{k}_x]^2 - k_0[\boldsymbol{\varepsilon}] \\ \mathbf{0} & -[\mathbf{K}_z] & -\frac{1}{k_0}[\mathbf{k}_y]^2 + k_0[\boldsymbol{\varepsilon}] & \frac{1}{k_0}[\mathbf{k}_y][\mathbf{k}_x] \\ \frac{1}{k_0}[\mathbf{k}_x][\boldsymbol{\eta}][\mathbf{k}_y] & -\frac{1}{k_0}[\mathbf{k}_x][\boldsymbol{\eta}][\mathbf{k}_x] + k_0 & -[\mathbf{K}_z] & \mathbf{0} \\ \frac{1}{k_0}[\mathbf{k}_y][\boldsymbol{\eta}][\mathbf{k}_y] - k_0 & -\frac{1}{k_0}[\mathbf{k}_y][\boldsymbol{\eta}][\mathbf{k}_x] & \mathbf{0} & -[\mathbf{K}_z] \end{pmatrix}. \quad (11)$$

Solving the eigenvalue problem in Eq. (10) gives us the wavevectors of the photonic crystal modes in the z direction (i.e., k_z) as eigenvalues, and the corresponding amplitudes of the Bloch components (i.e., $[\mathbf{U}_x, \mathbf{U}_y, \mathbf{S}_x, \mathbf{S}_y]^T$) as eigenvectors. Applying the boundary conditions afterward gives us the amplitudes for the reflected and the transmitted modes.

Note that for the case where the interface of the PC (chosen to be the x - y plane, without loss of generality) contains two of the PC lattice vectors (which is the case in most practical situations), the third reciprocal lattice vector, \mathbf{K}_3 , will be along the z direction, and this eigenvalue problem is redundant. Thus, if k_{zf} is a solution, so is $k_{zf} + nK_3$ (n being any integer number). This is the case that we will be considering in what follows.

There are two conditions that a PC mode has to satisfy to be considered as one of the possible modes excited inside the PC. First, the direction of energy for that mode should be away from the interface. Second, the amplitude of the mode should not grow toward infinity as the mode propagates. Moreover, considering the redundancy in the modes calculated in the previous section (wave vectors differing by a multiple of a reciprocal lattice vector represent the same PC mode), only $2N_1N_2$ modes are eligible to be included in the mode matching process (N_1 and N_2 are the numbers of Bloch components retained in the plane-wave expansion corresponding to the \mathbf{K}_1 and \mathbf{K}_2 reciprocal lattice vectors, respectively).

To enforce the condition of finite fields at infinity, only those modes with a nonnegative imaginary part of the wave vector are kept as the admissible modes. To calcu-

late the direction of energy of each mode, in the first step, we need to calculate the Poynting vector for each of the PC modes calculated in Section 1 using

$$\mathbf{P}_k = \frac{1}{2}\mathbf{E}_k \times \mathbf{H}_k^*, \quad (12)$$

where the subscript \mathbf{k} denotes the wave vector of the PC mode of interest. The Poynting vector normal to the interface can be calculated as

$$P_z = \frac{1}{2\omega} \{-\mathbf{U}_y^T \mathbf{S}_x + \mathbf{U}_x^T \mathbf{S}_y\}. \quad (13)$$

The sign of the Poynting vector determines whether the mode has its power propagating toward or against the interface. Only those PC modes which take power away from the interface are physically acceptable according to power conservation requirement. Thus, we retain $2N_1N_2$ PC modes, which are not redundant and satisfy the causality condition, in the PC region. In the incident region, in addition to the incident plane wave, we consider N_1N_2 plane waves with transverse electric (TE) polarizations, and N_1N_2 plane waves with transverse magnetic (TM) polarizations for the reflected orders from the PC structure. Therefore, the field matching equations can then be written as

$$\delta_{lm,00}U_{i,00x} + U_{r,lmx}^{\text{TE}} + U_{r,lmx}^{\text{TM}} + \sum_{t=1}^{2N_1N_2} a_t \sum_n U_{t,lmnx} \exp[-j(k_{zt} + nK_z)z_0], \quad (14)$$

$$\begin{aligned} & \delta_{lm,00}U_{i,00y} + U_{r,lm_y}^{\text{TE}} + U_{r,lm_y}^{\text{TM}} \\ &= \sum_{t=1}^{2N_1N_2} a_t \sum_n U_{t,lmny} \exp[-j(k_{zt} + nK_z)z_0], \end{aligned} \quad (15)$$

$$\begin{aligned} & \delta_{lm,00}S_{i,00x} + S_{r,lm_x}^{\text{TE}} + S_{r,lm_x}^{\text{TM}} \\ &= \sum_{t=1}^{2N_1N_2} a_t \sum_n S_{t,lmnx} \exp[-j(k_{zt} + nK_z)z_0], \end{aligned} \quad (16)$$

$$\begin{aligned} & \delta_{lm,00}S_{i,00y} + S_{r,lm_y}^{\text{TE}} + S_{r,lm_y}^{\text{TM}} \\ &= \sum_{t=1}^{2N_1N_2} a_t \sum_n S_{t,lmny} \exp[-j(k_{zt} + nK_z)z_0], \end{aligned} \quad (17)$$

where $U_{i,00x}$ and $U_{i,00y}$ denote the amplitudes of the x and y components of the magnetic field of the incident wave, respectively. Similarly, the x and y components of the incident electric field are represented by $S_{i,00x}$ and $S_{i,00y}$. The electric and magnetic field components of the different reflected orders (represented by lm , with $1 \leq l \leq N_1$ and $1 \leq m \leq N_2$) are denoted by $S_{r,lmv}$ and $U_{r,lmv}$ ($v=x,y$), respectively, and the superscript (TE or TM) denotes the polarization. Similar notation has been used for the transmitted electric and magnetic components of each transmitted PC mode (i.e., $S_{t,lmnx}$, $S_{t,lmny}$, $U_{t,lmnx}$, and $U_{t,lmny}$). Furthermore, $\delta_{lm,00}$ is the Kronecker delta function defined as $\delta_{lm,00}=1$ for $l=m=0$, and $\delta_{lm,00}=0$ otherwise. Finally, a_t represents the excitation amplitude of each PC mode inside the PC. Note that in Eqs. (14)–(17) the x and y variations of the phase terms are eliminated by applying the phase matching condition at the $z=z_0$ boundary. Without loss of generality, the TE and TM components of the reflected plane waves in Eqs. (14)–(17) are defined such that

$$\mathbf{S}_{r,lm}^{\text{TE}} \parallel (k_{r,lmx}\hat{\mathbf{x}} + k_{r,lmy}\hat{\mathbf{y}}) \times \hat{\mathbf{z}}, \quad (18)$$

$$k_0 \mathbf{U}_{r,lm}^{\text{TE}} = \mathbf{k}_{r,lmx} \times \mathbf{S}_{r,lm}^{\text{TE}}, \quad (19)$$

$$\mathbf{U}_{r,lm}^{\text{TM}} \parallel (k_{r,lmx}\hat{\mathbf{x}} + k_{r,lmy}\hat{\mathbf{y}}) \times \hat{\mathbf{z}}, \quad (20)$$

$$k_0 n_1^2 \mathbf{S}_{r,lm}^{\text{TM}} = \mathbf{U}_{r,lm}^{\text{TM}} \times \mathbf{k}_{r,lmx}, \quad (21)$$

in which

$$k_{r,lmz} = \sqrt{n_1^2 k_0^2 - k_{r,lmx}^2 - k_{r,lmy}^2}. \quad (22)$$

By solving the linear system of equations in Eqs. (14)–(17), we obtain the amplitudes of the reflected plane waves as well as the amplitudes of the PC modes excited in the PC region. In the rest of this paper, we will use this formulation to analyze reflection at the interface of different PC structures and to assess the accuracy of the approximate semianalytical model developed in Section 3.

Figure 1(b) shows schematically a tetragonal woodpile structure that can be fabricated through direct laser writing in a polymer material. The calculated reflection spectra for both TE and TM incident polarizations are shown in Fig. 2. Different plots in Fig. 2 correspond to different incident polarizations (TE or TM) and different incident medium (either air with $\epsilon_r=1.0$ or the substrate region

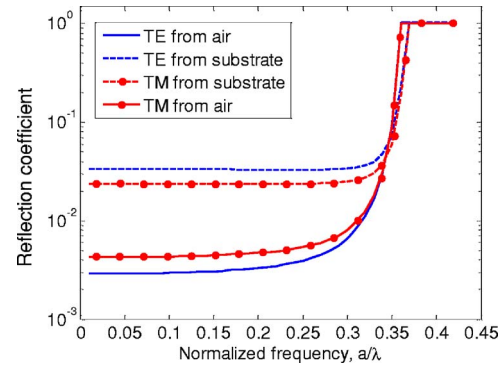


Fig. 2. (Color online) Power reflection coefficient at the interface of a tetragonal woodpile PC structure, as shown in Fig. 1(a), with $\epsilon_r=2.5$, $f_x=f_y=0.3$, $f_z=0.5$, $a_x=a_y=a$, and $a_z=1.2a$ is shown with $z_0=0$, and the incident planewave at $\alpha=5^\circ$ and $\phi=0^\circ$. Two cases with TE and TM polarizations (for the incident plane wave with electric field and magnetic field along the y direction) are considered with the incident plane wave coming either from air ($\epsilon_r=1.0$) or substrate ($\epsilon_r=2.5$).

with $\epsilon_r=2.5$). In these calculations, we have assumed an incoming plane wave with an incident angle of 5° [i.e., $\alpha=5^\circ$ and $\phi=0^\circ$ in Fig. 1(a)]. In our simulations, we have used $N_1=N_2=N_3=7$ plane-wave components for the expansion of the periodic variation of the PC mode in each direction. For this number of plane waves in the expansion, the calculated reflectance values obtained have an error of less than 5% in the reflected order powers. This error is calculated by estimating the exact value at each point through extrapolating the values as the number of plane waves in the calculations increases, and gives us enough accuracy for most practical applications. In the results plotted in Fig. 2, complete reflection ($\sim 100\%$) is observed at a range of frequencies (above $a/\lambda=0.35$ for incidence from air, and above $a/\lambda=0.36$ for incidence from the substrate), which corresponds to a stop band of the PC structure. Note that the slight difference between the range of stop bands for different incident regions is caused by the difference between the incident wave vectors (and thereby, the excitation wave vector) at different frequencies.

3. EFFECTIVE IMPEDANCE MODEL

Analysis of reflection using the rigorous method provided in Section 2 can provide an exact solution [for large values of N_1 , N_2 , and N_3 in Eqs. (6) and (7)] for the reflection at the interface of a 3D PC. However, the process is computationally intense and provides limited insight into the process of reflection at the interface of the PC. Such insights are very useful in designing buffer stages at the interface to minimize reflection [17]. We have previously proposed an effective impedance model for the analysis of reflection at the interface of 2D PCs [17]. The effective impedance model suggests that the continuity of field and conservation of power at the interface are needed for an impedance matching condition (to couple the light efficiently into or out of a PC structure). Here, we extend this model to the 3D case to analyze reflection at the interface of 3D PCs. For simplicity, we consider a TM-polarized in-

cident wave (with the magnetic field perpendicular to the plane of incidence), and define the effective impedance for a PC mode as

$$\eta_{PC} = \frac{2P_n}{\langle H_{int} \rangle^2}, \quad (23)$$

where $\langle H_{int} \rangle$ is the spatial average of the tangential magnetic field of the PC mode along the interface, and P_n is the Poynting vector of the mode normal to the interface. Here, we use the plane-wave expansion technique to find the mode of the structure for calculating its corresponding effective impedance at a specific interface. Using this effective impedance to represent the PC mode and assuming single-mode operation at both the incident medium and the PC region, we can define the reflection coefficient from the PC interface as

$$R = \left| \frac{\eta_{PC} - \eta_{inc}}{\eta_{PC} + \eta_{inc}} \right|^2, \quad (24)$$

where $\eta_{inc} = \sqrt{\mu_{inc}/\epsilon_{inc}}$ is the impedance of the homogeneous incident region with permittivity ϵ_{inc} and permeability μ_{inc} .

While the single-mode assumption here might seem too restrictive, it is usually desired for the proper operation of the PC structure for all practical applications of interest (e.g., wavelength demultiplexing, beam shaping, self-guiding, slow-light propagation, etc.). As an example, in low-contrast 3D PCs usually more than one mode are present, but the polarization of the incident wave can be selected such that excitation of other modes is negligible. It is also important to note that the effective impedance is defined for each PC mode and it depends on the interface at which the PC is truncated. Therefore, by choosing the incident region or a different termination of the PC, it is possible to realize an impedance matching condition to couple the light completely into the PC structure (with no reflection).

Figure 3(a) shows the calculated reflection for a plane-wave incident from a bulk medium with $\epsilon_r=2.5$ to a tetragonal woodpile PC with $a_x=a_y=a$, $a_z=1.2a$, $f_x=f_y=0.3$, and $f_z=0.5$ (parameters as defined in Fig. 1) with TM incident polarization at incident angles of $\alpha=7^\circ$ and $\phi=0^\circ$; the interface of the PC is assumed to be at $z_0=0.75a_z$ (i.e., halfway through the dielectric bars in the y direction). Both results from the rigorous mode-matching scheme and the effective impedance model are plotted in Fig. 3(a) and are in very good agreement. Figure 3(b) shows the effective impedance of the PC modes excited at different frequencies in Fig. 3(a). The impedance matching condition in this figure occurs around normalized frequency of $a/\lambda=0.337$, which corresponds to the complete transmission range in Fig. 3(a). Another important behavior in the effective impedance of PCs is that in the vicinity of the mode gap (depending on whether the average field goes to zero or a finite nonzero value), it is possible to obtain very large or very small values of effective impedance to match the PC modes of interest to the incident region.

Figure 4 shows the reflection of an incident wave from air at the interface of the PC analyzed in Fig. 3 for two different terminations at $z_0=0.25a_z$ and $z_0=0.75a_z$, along

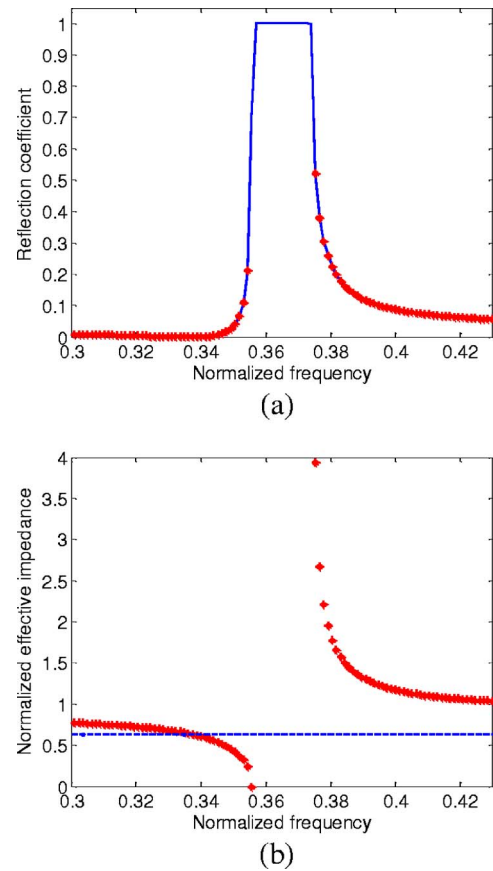


Fig. 3. (Color online) (a) Calculated reflection for a plane wave incident from a dielectric substrate ($\epsilon_r=2.5$) to a tetragonal woodpile PC with $a_x=a_y=a$, $a_z=1.2a$, $f_x=f_y=0.3$, and $f_z=0.5$ (parameters as defined in Fig. 1) with TM incident polarization (magnetic field along the y direction in Fig. 1) at an angle $\alpha=7^\circ$ is shown. The solid curve corresponds to the direct calculation results, and the star markers are those calculated using the effective impedance model. The interface of the PC is assumed to be at $z_0=0.75a_z$. (b) Calculated effective impedance (normalized to the impedance of the vacuum) of the PC in (a) is shown (marked by stars) and compared with that of the incident region (dashed line). Perfect impedance matching is observed at $a/\lambda=0.337$, and low reflection in the vicinity of that normalized frequency is consistent with the direct reflection calculation results.

with the calculated effective impedances. It can be seen that the behavior of the effective impedance is highly dependent on the choice of the interface. In particular, by controlling the location of the interface, it is possible to move the high-transmission region (in the vicinity of the impedance matching condition) to different frequency ranges for specific applications of interest.

4. DISCUSSION

The methods presented in this paper provide efficient tools for the analysis of reflection in PC structures. The rigorous technique based on the mode-matching concept is applicable under any condition (arbitrary PC, arbitrary incidence, and possibly with multimode incident or transmitted regions). The accuracy of this model can be controlled by changing the number of plane waves or PC modes used in the mode-matching process (which affects the size of the calculation matrices and thus, the overall

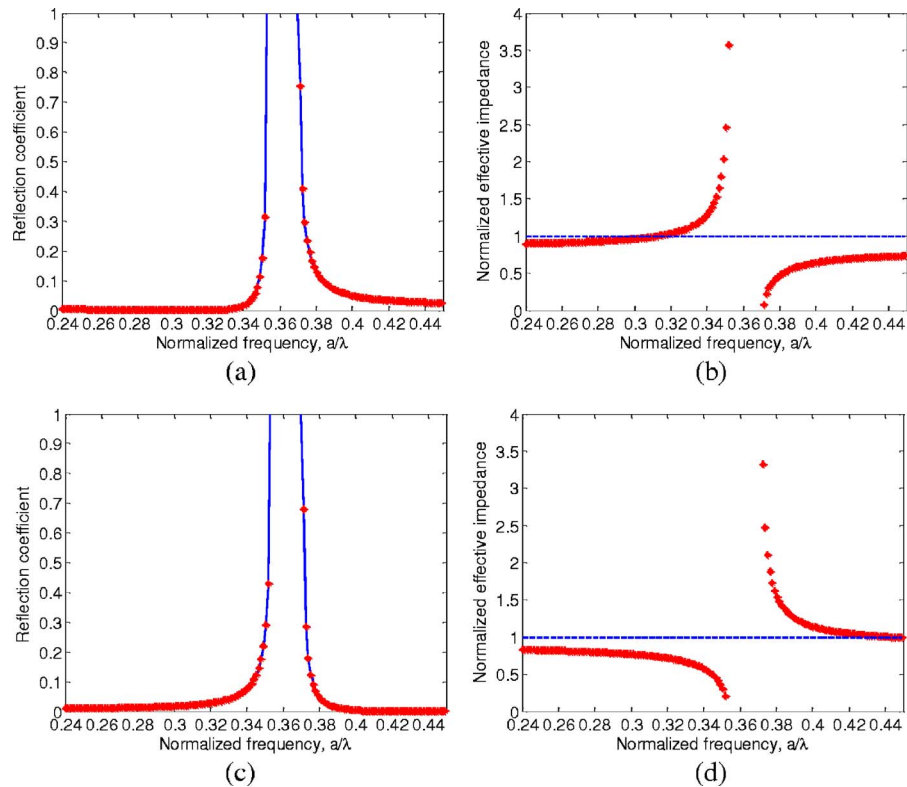


Fig. 4. (Color online) Calculated reflection for a plane wave incident from air ($\epsilon_r=1.0$) to the same tetragonal woodpile PC as in Fig. 3 with TM incident polarization at an angle $\alpha=7^\circ$ and $\phi=0^\circ$ is shown. The interface of the PC is assumed to be at $z_0=0.25a_z$ for the results plotted in (a), and the corresponding effective impedance is shown in (b). The calculated reflection and effective impedance for an interface at $z_0=0.75a_z$ are shown in (c) and (d), respectively. The dashed lines in (b) and (d) represent the normalized effective impedance of the incident region (i.e., air).

computation time). Therefore, it is a powerful tool for the numerical analysis of the most general PC structures. The disadvantage of this model is that it does not provide simple intuition for design and optimization of practical PC structures.

The effective impedance model presented here is a powerful tool for understanding and analysis of reflection in PC structures. The simulation time for this method is minimal compared to all existing techniques, as it requires only the calculation of the PC modes once (which is efficiently performed using only one unit cell of the PC structure). This mode calculation results can be used to find the effective impedance of the PC mode for all terminations of the PC (i.e., with the interface located at different positions relative to the unit cell of the PC) and for any permittivity in the incident region. This model also provides valuable insight for manipulation and optimization of reflection properties of the PC structures by relating the reflection to two well-known observable properties of PC modes, i.e., the field distribution and the Poynting vector of the PC mode. The single-mode requirement of the effective impedance approach is also required for the normal operation of the practical PC devices. Thus, we believe the results of this paper will be useful for minimization of reflection in practical PC structures.

5. CONCLUSIONS

We presented here two powerful and efficient methods for fast and accurate analysis of reflection at the interface of

3D PC structures. The rigorous mode-matching-based technique presented here is capable of analyzing reflection at the interface of any 3D PC structure with arbitrary bulk (or even periodic) media. On the other hand, the effective impedance method presented here is an accurate tool for the calculation of reflection at the boundary of single-mode 3D PC structures (or 3D PC structures with a dominant mode), which are in high demand for practical applications. The effective impedance model also provides valuable insight for the optimization of reflection at 3D PC interfaces with minimal computation need.

ACKNOWLEDGMENT

This work was supported by the Office of Naval Research under contract N00014-05-0303 (M. Spector).

REFERENCES

1. M. Loncar, T. Yoshie, J. Vuckovic, A. Scherer, H. Chen, D. Deppe, P. Gogna, Y. Qiu, D. Nedeljkovic, and T. P. Pearsall, "Nanophotonics based on planar photonic crystals," in *The 15th Annual Meeting of the IEEE LEOS* (IEEE, 2002), Vol. 2, pp. 671–672.
2. S. G. Romanov, P. Ferrand, M. Egen, R. Zentel, J. Ahopelto, N. Goponik, A. Eychmüller, A. Rogach, and C. M. Sotomayor Torres, "Exploring integration prospects of opal-based photonic crystals," *Synth. Met.* **139**, 701–704 (2003).
3. Y. C. Zhong, S. A. Zhu, H. M. Su, H. Z. Wang, J. M. Chen, Z. H. Zeng, and Y. L. Chen, "Photonic crystal with diamondlike structure fabricated by holographic lithography," *Appl. Phys. Lett.* **87**, 061103 (2005).

4. J. H. Moon, J. Ford, and S. Yang, "Fabricating three-dimensional polymeric photonic structures by multi-beam interference lithography," *Int. Symp. Polym. Adv. Technol.* **17**, 83–93 (2006).
5. J. H. Moon, S. Yang, and S.-M. Yang, "Photonic band-gap structures of core-shell simple cubic crystals from holographic lithography," *Appl. Phys. Lett.* **88**, 121101 (2006).
6. M. Deubel, G. von Freymann, M. Wegener, S. Pereira, K. Busch, and C. M. Soukoulis, "Direct laser writing of three-dimensional photonic-crystal templates for telecommunications," *Nat. Mater.* **3**, 444–447 (2004).
7. R. Guo, Z. Li, Z. Jiang, D. Yuan, W. Huang, and A. Xia, "Log-pile photonic crystal fabricated by two-photon photopolymerization," *J. Opt. A, Pure Appl. Opt.* **7**, 396–399 (2005).
8. M. Deubel, M. Wegener, S. Linden, G. von Freymann, and S. John, "3D–2D–3D photonic crystal heterostructures fabricated by direct laser writing," *Opt. Lett.* **31**, 805–807 (2006).
9. Y. Zeng, X. Chen, and W. Lu, "Electromagnetic modes in semi-infinite photonic crystals," *Physica E (Amsterdam)* **30**, 55–58 (2005).
10. T. P. White, C. M. De Sterke, R. C. McPhedran, and L. C. Botten, "Highly efficient wide-angle transmission into uniform rod-type photonic crystals," *Appl. Phys. Lett.* **87**, 111107 (2005).
11. Y.-C. Hsue and T.-J. Yang, "Applying a modified plane-wave expansion method to the calculations of transmittivity and reflectivity of a semi-infinite photonic crystal," *Phys. Rev. E* **70**, 016706 (2004).
12. Z.-Y. Li and K.-M. Ho, "Light propagation in semi-infinite photonic crystals and related waveguide structures," *Phys. Rev. B* **68**, 155101 (2003).
13. E. Istrate, A. A. Green, and E. H. Sargent, "Behavior of light at photonic crystal interfaces," *Phys. Rev. B* **71**, 195122 (2005).
14. X. Yu and S. Fan, "Anomalous reflections at photonic crystal surfaces," *Phys. Rev. E* **70**, 055601 (2004).
15. E. Schonbrun, Q. Wu, W. Park, T. Yamashita, and C. J. Summers, "Polarization beam splitter based on a photonic crystal heterostructure," *Opt. Lett.* **31**, 3104–3106 (2006).
16. X. Ao, L. Liu, L. Wosinski, and S. He, "Polarization beam splitter based on a two-dimensional photonic crystal of pillar type," *Appl. Phys. Lett.* **89**, 171115 (2006).
17. B. Momeni, A. A. Eftekhar, and A. Adibi, "Effective impedance model for analysis of reflection at the interfaces of photonic crystals," *Opt. Lett.* **32**, 778–780 (2007).